iScience

CellPress
OPEN ACCESS

Article

Transcriptomic response of wetland microbes to root influence

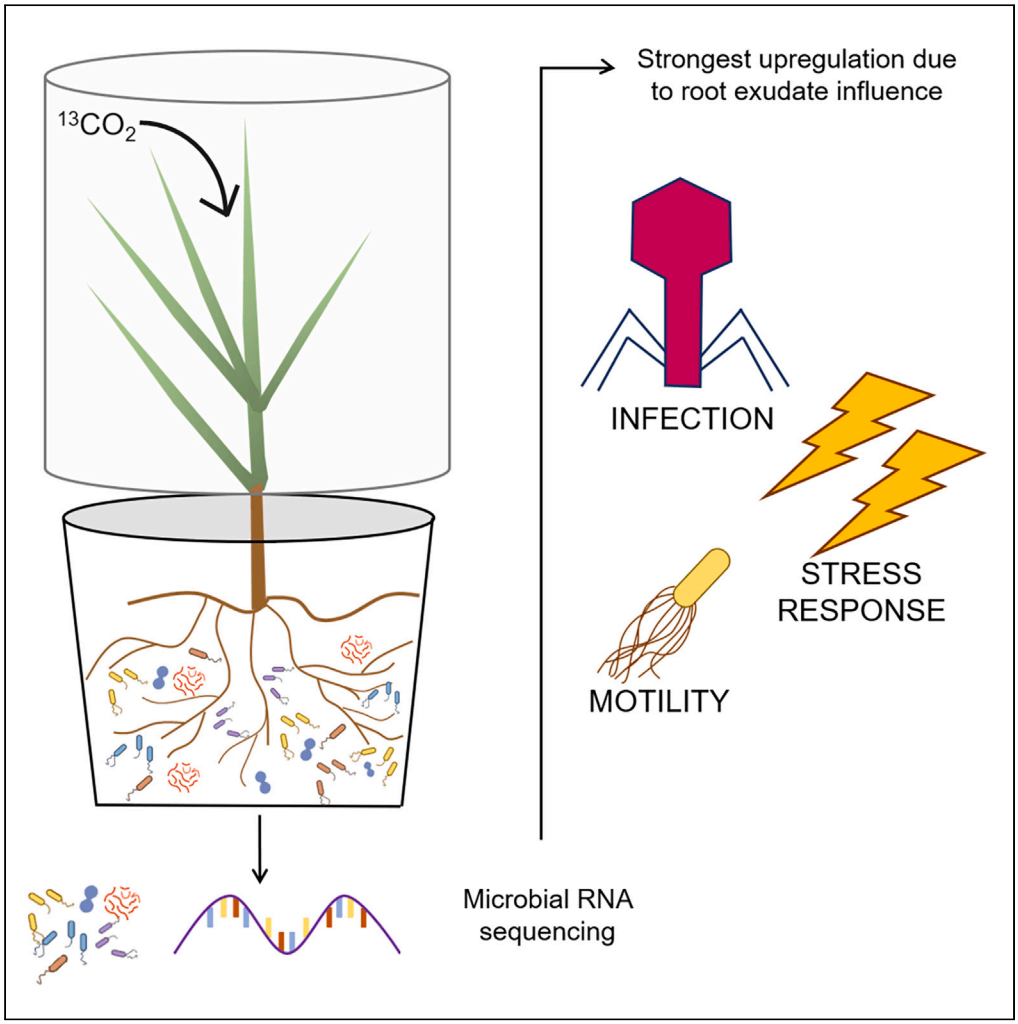

Luise Grüterich, Monica Wilson, Kai Jensen, Wolfgang R. Streit, Peter Mueller

luise.grueterich@uni-hamburg.de (L.G.)
mueller.p@uni-muenster.de (P.M.)

Highlights

Root exudates strongly stimulate microbial gene transcription

Plants strongly upregulate microbial infection, stress response, and motility pathways

Wetland soils favor the Wood-Ljungdahl pathway and dissimilatory sulfate reduction under anoxic conditions

Active microbial community composition changes under root exudate influence

Grüterich et al., iScience 27, 110890
November 15, 2024
https://doi.org/10.1016/j.isci.2024.110890

iScience

CellPress
OPEN ACCESS

Article

Transcriptomic response of wetland microbes to root influence

Luise Grüterich,[1,3,4,*] Monica Wilson,[1,3] Kai Jensen,[1] Wolfgang R. Streit,[1] and Peter Mueller[2,*]

SUMMARY

Wetlands are hotspots for carbon and nutrient cycling. The important role of plant-microbe interactions in driving wetland biogeochemistry is widely acknowledged, prompting research into their molecular biological basis for a deeper understanding of these processes. We analyzed transcriptomic responses of soil microbes to root exudates in coastal wetland soils using $^{13}CO_2$ pulse labeling. Metatranscriptomics revealed 388 upregulated and 11 downregulated genes in response to root exudates. The Wood-Ljungdahl pathway and dissimilatory sulfate reduction/oxidation were the most active microbial pathways independent of root influence, whereas pathways with the strongest upregulation in response to root influence were related to infection, stress response, and motility. We demonstrate shifts within the active community toward higher relative abundances of Betaproteobacteria, Campylobacterota, Kiritimatiellota, Lentisphaerota, and Verrucomicrobiota in response to exudates. Overall, this study improves our mechanistic understanding of wetland plant-soil microbe interactions by revealing the phylogenetic and transcriptional response of soil microorganisms to root influence and exudate input.

INTRODUCTION

The rhizosphere is defined as the volume of soil influenced by root activity.[1] Roots influence the physical and chemical properties of the soil matrix, the availability of soil resources (e.g., water and dissolved nutrients), and the activity of soil biota within the rhizosphere. The extent of root influence is a heterogeneous continuum that is characterized by strong biological, physical, and chemical gradients.[2,3] These gradients are produced by a complex array of factors, including biota-mediated processes such as rhizodeposition, root and microbial respiration, plant nutrient uptake, microbial signaling, and microbial degradation.[4,5] Strong biotic interactions between plant roots and soil biota to access limited soil resources make the rhizosphere a hotspot for biological activity and element exchange.[6,7]

Rhizodeposition is a key process shaping plant-soil microbe interactions in the rhizosphere.[8] While rhizodeposits encompass all root-derived organic inputs that enter the soil matrix regardless of origin and release mechanism,[9] primary and secondary metabolites released from intact, living roots, i.e., root exudates,[10] are particularly strong drivers of the microbial community.[11–13] Root exudates include low-molecular-weight compounds (e.g., sugars, amino acids, and organic acids)[14] and secondary metabolites (e.g., phenolics, flavonoids, and terpenoids)[15] as well as high-molecular-weight compounds (e.g., polymer-rich mucilage and proteins). Long-term tracer studies using isotopically labeled CO_2, e.g., continuous labeling, have been conducted to quantify net rhizodeposition.[16–18] However, pulse labeling, applied over short periods, is best suited to trace the fraction of new assimilates,[9,19] dominated by low-molecular-weight compounds via root exudation into the rhizosphere.[20,21]

There are a number of favorable and adverse effects of root exudates on soil microbial communities.[22] These biotic interactions are enabled through complex chemical signaling both to and from the roots.[23–25] Root exudates provide carbon- and energy-rich metabolic substrates for microorganisms in an otherwise carbon-limited environment. The input of carbon and increased soil respiration can shift the microbial community composition toward rapidly growing bacteria, *r*-strategists.[26] Numerous studies have demonstrated that the plant-controlled recruitment of rhizosphere microorganisms such as plant growth-promoting bacteria[27] and symbiotic mycorrhizal fungi[17] is regulated by root exudates.[28,29] Additionally, the exudation of secondary metabolites, antimicrobial compounds or chemo-attractants can be seen as a plant-defense mechanism to suppress pathogenic microbial groups.[30,31] Finally, plant-derived B-vitamins and other metabolites can affect the growth of soil microbes.[32,33]

The majority of rhizosphere studies on plant-soil microbe interactions has been conducted in upland terrestrial soil systems, with a particular focus on crops in agricultural soils. Studies on the rhizospheres of legumes,[34,35] wheat,[36] barley,[16,37] and maize[38,39] have revealed many

[1]Institute of Plant Science and Microbiology, University of Hamburg, Ohnhorststraße 18, 22609 Hamburg, Germany
[2]Institute of Landscape Ecology, University of Münster, Heisenbergstraße 2, 48149 Münster, Germany
[3]These authors contributed equally
[4]Lead contact
*Correspondence: luise.grueterich@uni-hamburg.de (L.G.), mueller.p@uni-muenster.de (P.M.)
https://doi.org/10.1016/j.isci.2024.110890

aspects of rhizosphere biology, such as the quantitative estimation of rhizodeposition,[18,40,41] microbial substrate utilization,[42] nutrient competition between plants and soil biota,[43] and the regulation of rhizosphere processes under elevated temperature.[44] Yet, while there is a growing body of research refining our understanding of plant-soil microbe interactions in upland terrestrial soils, there remains a significant gap in our knowledge regarding the transferability of these findings to plant-soil microbe interactions in rhizospheres characterized by contrasting abiotic and biotic environmental conditions, such as those found in wetlands and marine sediments.[5,45] (Meta-)transcriptomic approaches are increasingly being used to elucidate key genes expressed in wetland plant-microbe interactions,[46–48] however, transcriptomic analysis of prokaryotes in wetland rhizospheres remains challenging[49] with markedly few studies available (e.g.,[48,50]).

Frequent flooding and waterlogging in wetland soils strongly reduces the availability of oxygen, thereby limiting terminal electron acceptors and leading to lower rates of major microbial metabolic pathways as well as a shift toward anaerobic metabolism compared to well-aerated upland soils.[51] The impact of oxygen limitation on metabolic diversity has been predominantly studied in hydric soils, given that anaerobic sites in upland systems are mainly restricted to the interior of aggregates.[52] However, in wetlands, microbial communities are constrained by both carbon substrates (i.e., electron donors) and the availability of oxygen or alternative terminal electron acceptors.[53] Thus, root exudates may cause fundamentally different plant-microbe interactions in wetland compared to upland soils.[54]

The present study aims to improve our mechanistic understanding of wetland plant-soil microbe interactions by studying the phylogenetic and transcriptional response of soil microorganisms to root influence and exudate input. Using $^{13}CO_2$ pulse labeling and carbon tracing, we analyzed the microbial response to root influence in the anoxic rhizosphere of the common coastal wetland grass *Spartina anglica*. In particular, we aimed to determine the influence of root exudation on microbial gene expression, identify which metabolic pathways are affected, understand which microbial taxonomic groups are primarily involved, and compare these responses to the bulk soil microbial community.

RESULTS

Microbial gene expression

$^{13}CO_2$ pulse labeling and carbon tracing were used to study the microbial response to root exudation by the common coastal wetland grass *Spartina anglica* under wetland-typical waterlogged conditions (Figure 1). A total of six metatranscriptomes of the bulk and rhizosphere microbiota (Tables S2 and S3) were studied. For each each group (i.e., bulk vs. rhizosphere), three independent biological replicates were analyzed. For all six metatranscriptomes, an average of 16 million reads was obtained. In total, 85,886 genes showed a minimum of 1 transcript.

After setting the *p*-value and $\log_2$-fold change significance thresholds (see STAR Methods section metagenome and metatranscriptome analysis), we observed that 388 of the resulting differentially expressed genes were significantly (adjusted $p < 0.05$) upregulated and 11 were significantly (adjusted $p < 0.05$) downregulated (Figure 2A) in response to root exudate influence. A principal component analysis (PCA) using normalized counts showed a clear distinction between the three replicates with high root exudate influence and the three replicates with no root exudate influence. The first principal component (PC1) explained 63% of the variance between the two depicted groups (Figure 2B).

Gene expression of the background microbial community

We conducted a key gene analysis on microbial processes independent of root exudate influence to establish the background environmental context of the bulk soil microbial community. This analysis examined the transcript abundances of indicator genes involved in carbon, nitrogen, and sulfur cycles (Figure 3A) (gene selection based on Yang et al.[55]).

Key genes of the Wood-Ljungdahl pathway (WLP) (*CODH/ACS*) and dissimilatory sulfate reduction/oxidation (DSR) (*sat*, *aprA*, *aprB*, *dsrB*) exhibited the highest transcript numbers across all investigated pathways independently of differential expression with transcript abundances of 4093 (*aprA*), 967 (*dsrA*), 1235 (*dsrB*) and 1170 (*CODH/ACS*) (Figure 3A). We dissected both WLP and sulfur metabolism into their constituent genes and examined their respective transcript abundances (Figures 3B and 3C). We observed that within these pathways some genes are higher transcribed than others. For the WLP the last two genes (*pta*, *ackA*), that are responsible for the conversion of acetyl-CoA to acetate, showed nearly no transcripts. Regarding sulfur metabolism, only the full gene repertoire for DSR showed notable transcript numbers.

To obtain further insight into which microbial groups drove sulfate metabolism and WLP, we performed a phylogenetic analysis. The top three microbial groups behind sulfate metabolism were Thermodesulfobacteriota with 34.7%, Gammaproteobacteria with 24% and Deltaproteobacteria with 10.7%. The main microbial groups involved in the WLP were Thermodesulfobacteriota with 66.7% and Deltaproteobacteria with 25%. Community composition analysis for the sulfate metabolism was based on all 75 gene entries assigned to sulfur metabolism key genes. Community composition analysis for the WLP was based on all 12 gene entries assigned to the WLP key genes.

Transcriptomic changes in response to root exudates

For 338 differentially expressed genes (adjusted $p < 0.05$), pathway annotation was possible. Notably, 327 of these genes were upregulated and only 11 were downregulated. These genes were sorted by functional categories into four pathway supercategories and 15 subcategories (listed in Table 1). 'Infection', 'Stress response', and 'Motility' showed with 7.3, 7.0, and 6.8 the highest $\log_2$-fold change median values indicating the strongest effect of root exudate influence on these pathway categories (Figure 5). Within the 'Stress response' and 'Transport' categories, genes associated with oxidative stress and iron transport showed strong upregulation. Rubrerythrin ($\log_2$-fold change = 8.54) and thioredoxin ($\log_2$-fold change = 6.63) were linked to oxidative stress, while the FecR protein ($\log_2$-fold change = 6.24) and TonB-dependent receptor ($\log_2$-fold change = 5.84) were linked to iron transport (Table S4, Queries: Gene184520, Gene169819, Gene12770, Gene015030).

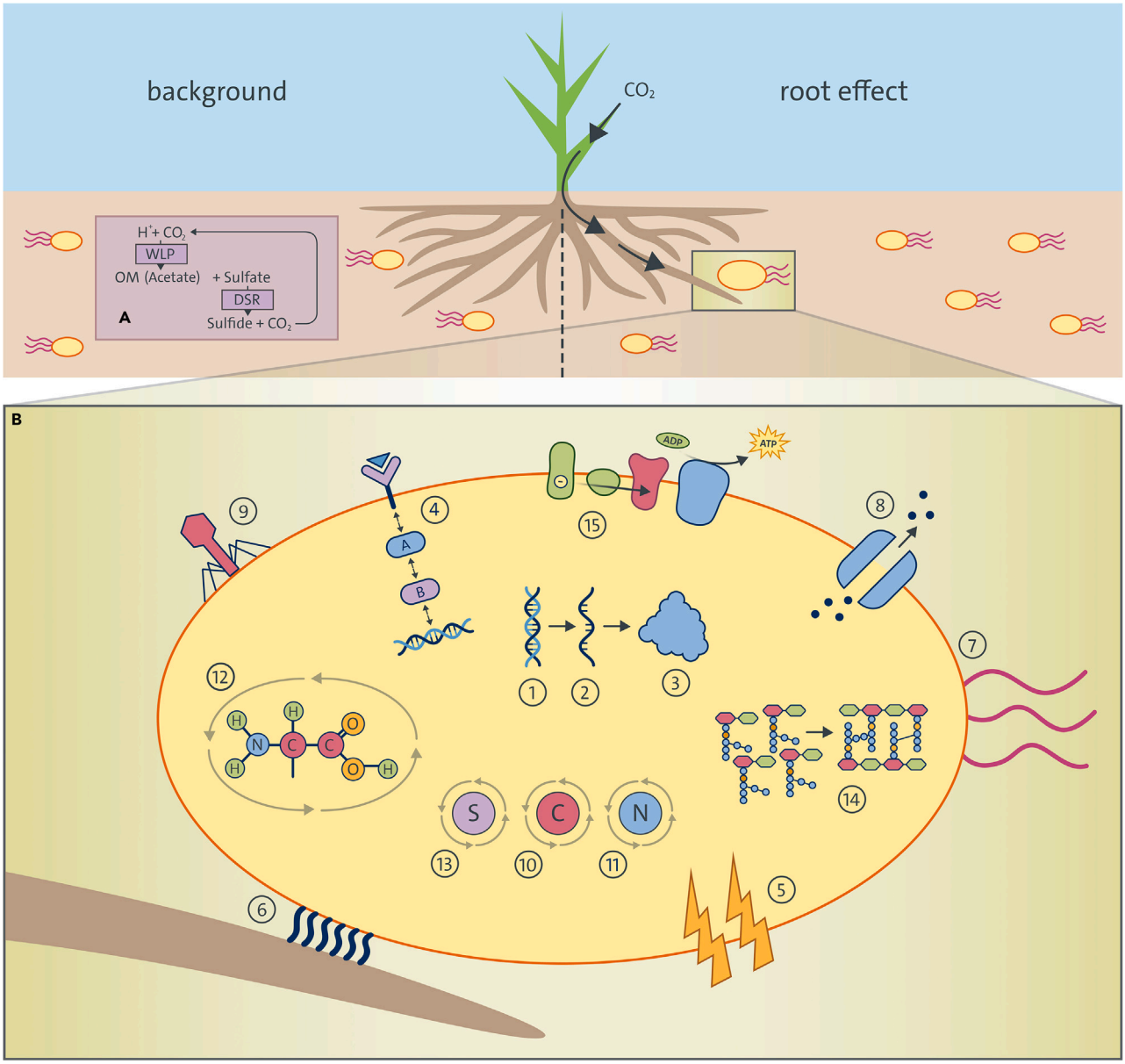

Figure 1. Differential gene expression in soil microbes under plant influence vs. independent conditions

Conceptual representation of upregulated microbial processes in response to plant influence (B) and independent of plant influence (A). Yellow objects represent the soil microbes. Independent of plant influence, key genes of the Wood-Ljungdahl pathway and dissimilatory sulfate reduction exhibit the highest transcript abundances (A). Frame B shows a zoom into one of the microbes influenced by exudate input. In response to exudate input, 338 genes show significant upregulation (adjusted $p < 0.05$) and can be categorized into the following metabolic pathways. 1) Transcription, 2) Translation, 3) Proteostasis, 4) Signal transduction and exchange, 5) Stress response, 6) Adhesion, 7) Motility, 8) Transport, 9) Infection, 10) Carbon metabolism, 11) Nitrogen metabolism, 12) Amino acid metabolism, 13) Sulfur metabolism, 14) Cell wall synthesis, and 15) Electron transport. Image by courtesy of UHH/Alpen.

Microbial community shifts

A phylogenetic analysis was conducted to assess the shifts in the community caused by the presence and absence of root exudates, respectively. Initially, we assigned phylogenetic classifications to all transcripts present in the soil. The most abundant microbial groups, namely Gammaproteobacteria and Thermodesulfobacteriota collectively accounted for 51.4% of all transcripts.

In relation to the 388 transcripts that exhibited significant upregulation due to the influence of root exudates (adjusted $p < 0.05$), notable changes were observed in the proportions of certain taxa. Specifically, the proportion of Betaproteobacteria increased from 1% to 15.3%, Campylobacterota increased from 0.6% to 1.8%, Kiritimatiellota from 0.8% to 13%, Lentisphaerota from 0.3% to 6.5%, and Verrucomicrobiota from 0.4% to 3.4%. 65.9% of all transcripts were assigned to Betaproteobacteria, Gammaproteobacteria, and Kiritimatiellota (Figure 6). Of the

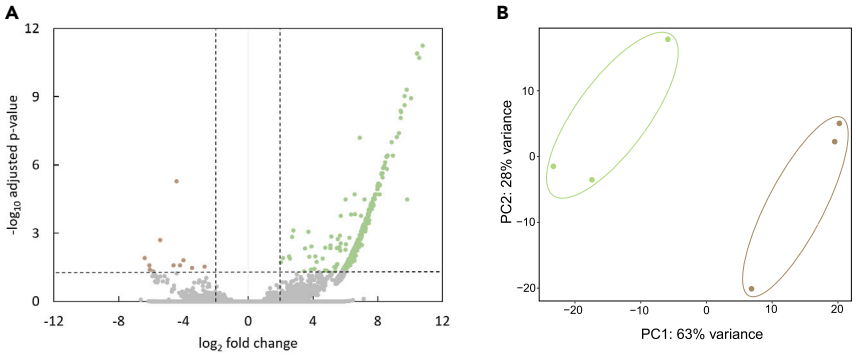

Figure 2. Volcano plot and PCA analysis of gene expression in response to root exudate influence in soil microbes

Volcano plot depicts all 85,886 genes with a minimum of 1 transcript assigned. An adjusted *p*-value <0.05 and a $\log_2$-fold change >2, < −2 were used as cutoff (dashed lines). Colored dots indicate genes with significant upregulation (green) or downregulation (brown) in response to root exudate influence. Gray dots indicate genes without significant differential expression (A). PCA using normalized counts shows a separation between the three replicates with high root exudate influence (green) and no root exudate influence (brown) (B).

upregulated genes assigned to Betaproteobacteria, the majority were categorized into the pathway groups of translation, motility, and transport. For Kiritimatiellota, these were carbon metabolism, translation, and transport. For Lentisphaerota, the upregulated pathway groups were carbon metabolism and translation and for Verrucomicrobiota, they were motility and transport.

DISCUSSION

This study offers insight into the wetland microbial response to root exudation via metatranscriptomic analysis. We identified both upregulated and downregulated microbial metabolic pathways in response to exudate input (Figure 1; Tables 1 and 2), shedding light on the complex plant-microbe interplay in wetland soils. We assigned the microbial taxonomic groups which reacted to root exudates and compared them to those groups driving bulk soil microbial processes (Figures 4 and 6). Notably, the upregulated fraction of genes was around 30-fold higher than the downregulated fraction.

Metabolic background of soil microbes independent of differential expression

We acquired metatranscriptomic data on microbial processes independent of root exudate influence (Figure 1A) to establish the background environmental context of the bulk soil microbial community subjected to root influence (Figures 1A and 1B).

The WLP and DSR were the primary metabolic pathways in the plant-independent soil microbial community of the bulk soil (Figure 3). It has been demonstrated in upland beech and pine forest soils that the WLP was one of the least dominant autotrophic pathways predicted.[56] Furthermore, in (semi-)arid soils, it has been shown that the WLP had the lowest relative abundance of key genes compared to the other CO_2 fixing pathways.[57] This study demonstrates that anaerobic wetland soils, in contrast, create conditions that favor the WLP. The prominence of WLP and DSR transcripts indicate the active utilization of these pathways under anoxic conditions, with a preference for low ATP consumption.[58,59] While the dominance of sulfate reduction as an anaerobic microbial pathway in marine and coastal ecosystems is long established,[60–62] recent metatranscriptomic work from our group also demonstrate a high prevalence of dark CO_2 fixation via WLP in the anoxic soils of these ecosystems.[63] WLP and DSR are interconnected or mutually beneficial pathways, because the end-product of the WLP, acetate, can flow into the DSR as carbon and energy source.[60] Conversely, the DSR end-product, CO_2, can serve as carbon source in the WLP (Figure 1A). It is therefore possible that a single bacterial species or organism is making use of both processes.[64] Indeed, our data show that Thermodesulfobacteriota and Deltaproteobacteria are associated with transcripts related to both DSR and WLP (Figure 4) and reveal several species transcribing for both WLP and DSR key genes at high frequencies.

The high transcription of *fhs* and *CODH/ACS* indicates high abundances of acetogenic bacteria that typically utilize the acetyl-CoA pathway to produce acetate as an end-product.[65] However, low transcriptional levels of genes responsible for converting acetyl-CoA to acetate (*pta* and *ackA*, Figure 3B) may indicate anabolic incorporation of acetyl-CoA as the primary metabolic process, possibly reflecting a strategy to conserve energy. Acetyl-CoA is essential in various metabolic pathways, including CO_2 fixation pathways,[66] potentially making it more energy-efficient to channel it directly into other metabolic processes rather than converting it to acetate.

Anoxic, sulfate-rich wetland soils promote Deltaproteobacteria, Gammaproteobacteria and Thermodesulfobacteriota to be the drivers behind the main active microbial pathways, namely DSR and WLP (Figure 4). Gammaproteobacteria are known to be abundant in anoxic environments[67,68] and increase in abundance toward marine conditions.[69] The abundance of methanogenic microbial groups and transcripts encoding for methanogenesis was negligible in our study (Figure 3A). This high prevalence and activity of sulfate-reducing bacteria in comparison to methanogens is often explained by the higher free energy yield of sulfate reduction in relation to methanogenesis,[51] which allows sulfate reducers to outcompete methanogens for energy or carbon substrates, such as H_2 and acetate in sulfate-rich environments typically observed in coastal and marine ecosystems.[70–72]

A

	genes	average transcript abundance
Denitrification	*nosZ*	9
	norB	3
	nirk	0
	nirS	4
	napA	22
	narG	6
Dissimilatory nitrate reduction	*nirB*	8
	nrfA	10
Methanogenesis	*mcrA*	0
Methylotrophy	*mdo*	0
Nitrification	*amoA*	0
	hao	0
Nitrogen fixation	*nifD*	1
	nifH	3
	nifk	2
Sulfur metabolism	*aprA*	4093
	dsrA	967
	dsrB	1235
Thiosulfate oxidation	*soxA*	4
	soxB	57
	soxY	34
Wood-Ljungdahl pathway	*CODH/ACS*	1170
rTCA cycle	*aclAB*	0
Calvin cycle	*cbbL*	62
	rbcS	5
DC/4-HB cycle	*abfD*	0
3-HP bicycle	*accD*	22
	PCCB	5
3-HP/4-HB cycle	*Msed_2001*	0
Fructose degradation	*xylA*	26
Glycolysis	*pfkA*	58
	pyk	105
Pentose phosphate pathway	*gnd*	33

B

Wood-Ljungdahl pathway	genes	average transcript abundance
formate dehydrogenase	*fdhA*	223
formyl-THF synthetase	*fhs*	3063
formyl-THF cyclohydrolase	*folE*	45
methylene-THF dehydrogenase	*folD*	263
methylene-THF reductase	*metF*	144
methyltransferase	*aceE*	141
CO dehydrogenase/acetyl-CoA synthase	*CODH/ACS*	1170
phosphotransacetylase	*pta*	38
acetate kinase	*ackA*	19

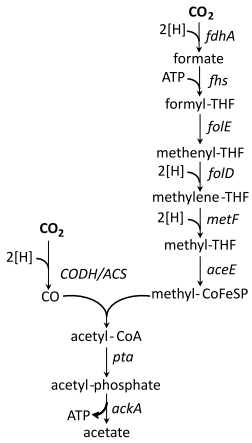

C

Sulfur metabolism

Assimilatory sulfate reduction	*sat*	812
	cysNC	59
	cysH	7
	cysIJ	11
Dissimilatory sulfate reduction/oxidation	*sat*	812
	aprA	4093
	aprB	1066
	dsrA	967
	dsrB	1235
SOX system	*soxA*	4
	soxB	57
	soxC	5
	soxD	1
	soxX	17
	soxY	34
	soxZ	3

Figure 3. Average transcript abundance of key genes in carbon, nitrogen, and sulfur cycles

Average transcript abundance based on $n = 6$ metatranscriptomes of selected key genes of carbon, nitrogen, and sulfur cycles (A), entirety of genes involved in the WLP (B), and entirety of genes involved in sulfur metabolism (C). See also Table S4.

Root activity-driven change in expression of soil microbial genes

The three replicates with root exudate influence and the three replicates without root exudate influence show a clear distinction in the expression of soil microbial genes (Figure 2B). The majority of differentially expressed genes is upregulated in response to root exudate influence (Figure 2A). This observation implies a strong stimulatory effect of the various plant exudates on the microorganisms and their metabolism that can be attributed to few pathway categories (Figure 5; Table 1). The metabolic categories with the strongest microbial response to root exudates were assigned to infection ($\log_2$-fold change = 7.34), stress response ($\log_2$-fold change = 7.03), and motility ($\log_2$-fold change = 6.84) (Figure 5; Table 1). Notably, infection-related genes also include those involved in establishing plant-beneficial symbiotic interactions. Thereby, microorganisms (pathogens and non-pathogens) are able to sense the root presence using root exudates and prepare to infect the plant.[73,74]

Regarding stress response, genes can be part of defense mechanisms that microbes activate to protect themselves from toxic environmental influences. This could, for example, be a response to the release of secondary plant compounds, oxygen, or reactive oxygen species upon pathogen recognition or response to abiotic stress.[75,76] Concerning motility, microbes direct their movement along chemical gradients in their environment and thus locate optimal conditions for growth and survival.[77] Microbial motility is also crucial for surface colonization and attachment to the root. The occurrence of transcripts relating to the cellular response to environmental stimuli, e.g., motility, aligns with findings from Wu et al.,[78] who also found motility, and additionally, polymer utilization to be enriched in the rhizosphere of maize, although, in contrast to our transcriptomic approach, their findings are based on metagenomics. Here, we demonstrated that also wetland plants influence the mobility of rhizosphere microbial communities.

Amino acid biosynthesis comes at a high cost for microorganisms and the corresponding biosynthesis pathways are tightly regulated. By utilizing amino acids via root exudates, soil microbes can save energy by abstaining from producing them internally. 3 of the 11 genes that were downregulated under the influence of root exudates were assigned to the glutamate dehydrogenase (Table 2). The glutamate dehydrogenase catalyzes the conversion of glutamate to α-ketoglutarate and ammonium. This reaction is important for further downstream synthesis of other amino acids. In the presence of high levels of exudate-derived compounds, microbes may favor the use of these compounds

Table 1. Functional categories for KEGG pathway enrichment analysis of significantly upregulated genes

Pathway supercategory	Pathway subcategory	Log_2-fold change	Queries (n)
Gene expression and regulation	Transcription	6.4	15
	Translation	6.1	51
	Proteostasis	6.3	24
Cellular processes in response to environmental stimuli	Signal transduction and exchange	6.0	7
	Stress response	7.0	11
	Adhesion	6.5	16
	Motility	6.8	31
	Transport	6.2	37
	Infection	7.3	10
Carbon, nitrogen and sulfur metabolism	Carbon metabolism	6.3	53
	Nitrogen metabolism	6.1	15
	Amino acid metabolism	6.1	25
	Sulfur metabolism	6.7	7
Cellular structure and energy supply	Cell wall synthesis	5.9	5
	Electron transport	6.5	31

List of functional categories for KEGG pathway enrichment analysis of 338 annotated gene queries with a significant upregulation (adjusted $p < 0.05$). Median log_2-fold change values are shown. See also Table S4.

over endogenous glutamate metabolism. By downregulating glutamate dehydrogenase, they can reduce competition for substrates and channel available resources toward other metabolic pathways that benefit from the exudates.[79]

The metabolic categories translation, transport, and carbon metabolism have the highest query numbers (Figure 5; Table 1). Upregulation of translation genes typically indicate increased protein synthesis or enhanced efficiency in the translation process in response to environmental changes.[80] Upregulated carbon metabolism genes indicate increased expression of proteins involved in utilizing carbon compounds, particularly in soils influenced by root exudates. Transport genes are upregulated to facilitate the movement of compounds between plant and microbial cells or the transport of enzymes for molecule degradation outside of the cell. Further, anaerobic wetland microbiota are known to rely on alternative terminal electron acceptors.[53] Input of molecular oxygen via radial oxygen loss from roots into reduced soils can provide terminal electron acceptors for the oxidation of reduced Fe(II).[51] Additionally, it has been demonstrated by Yang et al.,[81] that wetland plants tend to have high Fe concentrations on root surfaces and in their rhizosphere. Our data suggest that, for example, Fe(III) deposition resulting from the oxidation of Fe(II) at the oxic-anoxic interface may serve as terminal electron acceptor by Fe-reducers. Root exudates can acidify the surrounding soil and increase the mobility of iron,[82] which is supported by our observation of strong upregulation of genes directly related to iron transport in samples associated with high exudate influence (Table S4, Queries: Gene184520, Gene169819, Gene12770, Gene015030).

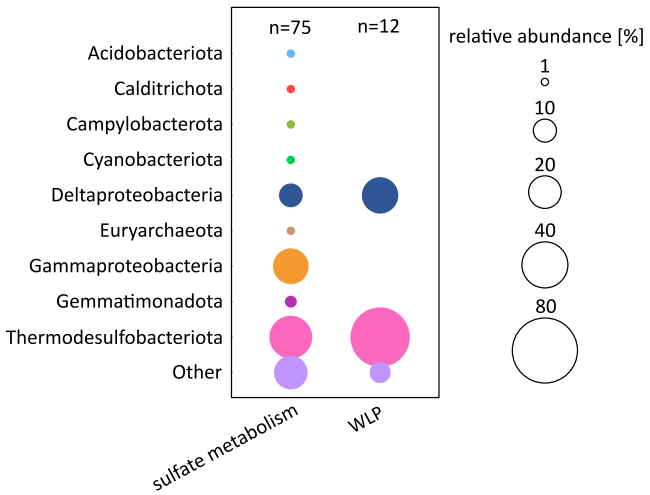

Figure 4. Microbial composition of sulfur metabolism and Wood-Ljungdahl pathway assigned transcripts

Microbial community composition based on transcripts of key genes assigned to sulfur metabolism (first column; $n = 75$) and based on transcripts of key genes assigned to the WLP (second column; $n = 12$).

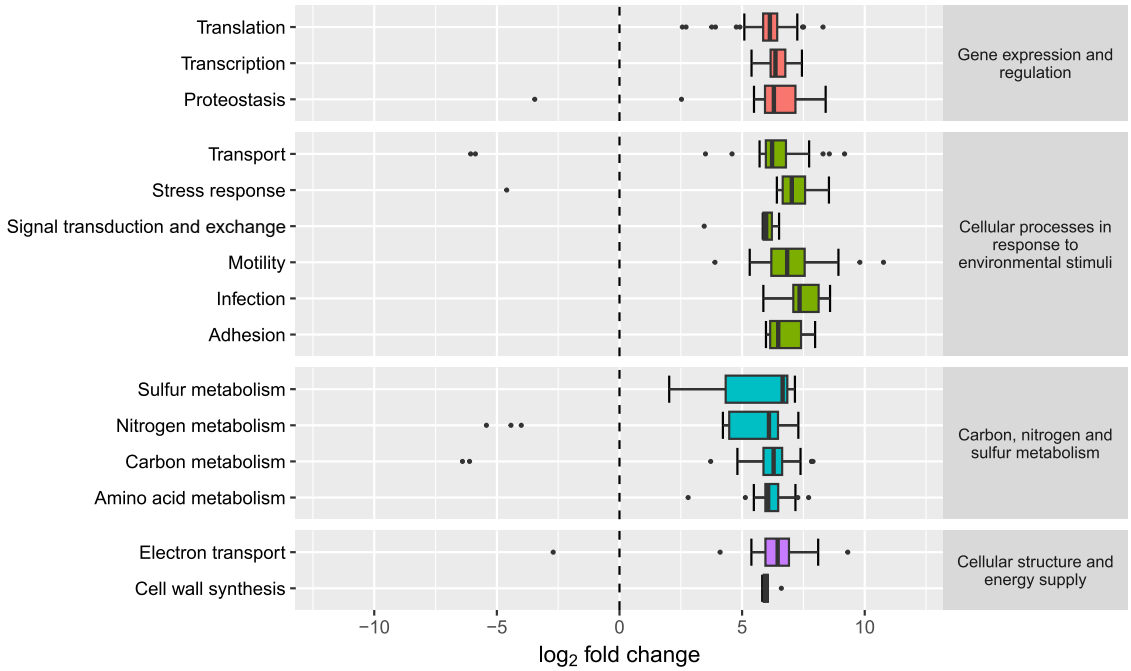

Figure 5. Boxplot of KEGG pathway enrichment analysis for significantly regulated genes under root exudate influence

Boxplot of KEGG pathway enrichment analysis for 338 annotated gene queries with a significant change in expression (adjusted $p < 0.05$) grouped by functional categories (Table 1). Positive $\log_2$-fold changes reflect upregulation and negative $\log_2$-fold changes reflect downregulation of genes due to root exudate influence. Outliers are displayed as individual points. See also Table S4.

Higher relative abundance of transcripts assigned to certain microbial groups in response to root exudates compared to the abundance of these groups in the bulk soil reflect more favorable conditions for these taxa in the short-term and potentially increased competitive advantage in the long-term. The microbial community that reacts to root exudates by upregulation of genes differs from the community based on all transcripts (Figure 6). Specifically, the relative abundance of Betaproteobacteria, Campylobacterota, Kiritimatiellota, Lentisphaerota, and Verrucomicrobiota increased based on assignment to upregulated genes due to root exudate influence (Figure 6). These results echo a similar metagenomic and metatranscriptomic rhizosphere study investigating rhizosphere effects of *Avena fatua* in a loamy upland soil,[83] in which Betaproteobacteria and Verrucomicrobiota also significantly increased in the rhizosphere relative to the bulk soil based on 16S cDNA.

Limitations of the study

Our experimental approach aimed to capture microbial responses to exudates beyond their role as a carbon source, thus differing from RNA-SIP (RNA-Stable Isotope Probing) approaches, which rely on the uptake and metabolic utilization of exudates. Microbes can respond to exudates by different mechanisms without necessarily metabolizing them. For example, microbes may sense exudates and invest in flagella to move closer to or away from them. Also, exudates can act as repellents, toxins, or inhibitors and influence microbial activity without directly serving as a carbon source. A drawback of our approach is, however, that it cannot clearly distinguish the effects of organic exudate release from those of other root processes, such as proton and oxygen release, as it uses a ^{13}C label to specifically track the exudate input to the soil. It is important to recognize that none of the currently available approaches alone are sufficient to fully capture the microbial response to exudates while excluding the influence of other root-related factors. To address this limitation, future research investigating microbial transcriptomic responses to root influence should assess options for combined approaches integrating multiple methods.

This study is further limited by its small sample size ($n = 3$ for each of 'background' and 'root affected' samples) and its focus on a single, albeit dominant and globally distributed plant species of coastal wetlands.[84] These constraints may limit the generalizability of our findings. Therefore, future research should investigate larger sample sizes and wider geographic coverage to confirm these results at a larger scale.

RESOURCE AVAILABILITY

Lead contact

Further information and requests for resources and reagents should be directed to and will be fulfilled by the lead contact, L.G. (luise.grueterich@uni-hamburg.de).

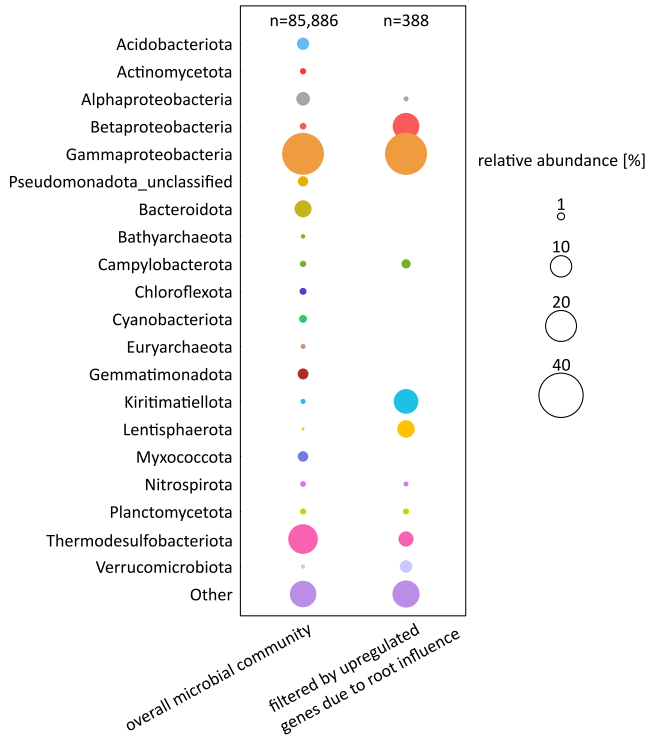

Figure 6. Microbial composition shift of root-influenced upregulated genes

Microbial community composition based on all transcribed genes (first column; n = 85,886) and based on transcribed genes upregulated due to root influence (second column; n = 388; adjusted $p < 0.05$).

Materials availability

This study did not generate new unique reagents.

Data and code availability

- Raw reads of the metagenomic and metatranscriptomic analysis have been deposited at the European nucleotide archive (ENA) and are publicly available as of the date of publication. Accession numbers are listed in the key resources table.
- This paper does not report original code.
- Any additional information required to reanalyze the data reported in this paper is available from the lead contact upon request.

Table 2. Functional categories for KEGG pathway enrichment analysis of significantly downregulated genes

Down regulated genes (Description)	Subcategory	Log_2-fold change
Glutamate dehydrogenase	Nitrogen metabolism	−5.4
Glutamate dehydrogenase (*gdhA*)	Nitrogen metabolism	−4.4
Glutamate dehydrogenase (*gluD*)	Nitrogen metabolism	−4.0
Phycobilisome protein (*apcA*)	Carbon metabolism	−6.4
Protein involved in exopolysaccharide biosynthesis	Carbon metabolism	−6.1
PFAM ABC transporter	Transport	−6.1
Predicted permease	Transport	−5.9
COG1842 Phage shock protein A (IM30) (*pspA*)	Stress response	−4.6
Peptidase S1C (*degP-2*)	Proteostasis	−3.4
NADH ubiquinone oxidoreductase (*nuoF2*)	Electron transport	−2.7
NA	NA	−4.2

List of functional categories for KEGG pathway enrichment analysis of 338 annotated gene queries with a significant negative change in transcript abundance, i.e., downregulation (adjusted $p < 0.05$). Median log_2-fold change values are shown. The downregulated genes shown in this table correspond to 11 gene queries. See also Table S4.

ACKNOWLEDGMENTS

This study was funded by the Deutsche Forschungsgemeinschaft (DFG, German Research Foundation) within the Research Training Group 2530 "Biota-mediated effects on Carbon cycling in Estuaries" at University of Hamburg (project number 407270017) and the DFG Emmy Noether project "Rhizosphere-mediation of biosphere-climate feedbacks" (project number 502681570) at University of Münster. We thank Simon Thomsen and Clarisse Gösele for designing and testing the labeling chamber used in our experiments. We furthermore thank GreenGate Genomics for bioinformatic services.

AUTHOR CONTRIBUTIONS

Conceptualization, P.M. and L.G.; Methodology, P.M., L.G., and M.W.; Investigation, L.G. and M.W.; Formal analysis, L.G. and M.W, Writing – Original Draft, L.G. and M.W.; Writing – Review and Editing, L.G., M.W., P.M., K.J., and W.S.; Resources, P.M., K.J., and W.S.; Supervision, P.M., K.J., and W.S.

DECLARATION OF INTERESTS

The authors declare no competing interests.

STAR★METHODS

Detailed methods are provided in the online version of this paper and include the following:

- KEY RESOURCES TABLE
- EXPERIMENTAL MODEL AND STUDY PARTICIPANT DETAILS
  - *Spartina anglica* plant cultivation
- METHOD DETAILS
  - $^{13}CO_2$ pulse labeling
  - Soil sample collection and ^{13}C enrichment analysis
  - RNA and DNA extraction from soil
  - Metatranscriptome and metagenome analysis
- QUANTIFICATION AND STATISTICAL ANALYSIS

SUPPLEMENTAL INFORMATION

Supplemental information can be found online at https://doi.org/10.1016/j.isci.2024.110890.

Received: March 31, 2024
Revised: June 17, 2024
Accepted: August 26, 2024
Published: September 17, 2024

REFERENCES

1. Hiltner, L. (1904). Über neuere Erfahrungen und Probleme auf dem Gebiete der Bodenbakteriologie unter besonderer Berücksichtigung der Gründüngung und Brache. Arbeiten der Deutschen Landwirtschaftlichen Gesellschaft *98*, 59–78.
2. Koop-Jakobsen, K., Mueller, P., Meier, R.J., Liebsch, G., and Jensen, K. (2018). Plant-Sediment Interactions in Salt Marshes - An Optode Imaging Study of O_2, pH, and CO_2 Gradients in the Rhizosphere. Front. Plant Sci. *9*, 541. https://doi.org/10.3389/fpls.2018.00541.
3. Koop-Jakobsen, K., Meier, R.J., and Mueller, P. (2021). Plant-mediated rhizosphere oxygenation in the native invasive salt marsh grass Elymus athericus. Front. Plant Sci. *12*, 669751. https://doi.org/10.3389/fpls.2021.669751.
4. Kuzyakov, Y., and Razavi, B.S. (2019). Rhizosphere size and shape: Temporal dynamics and spatial stationarity. Soil Biol. Biochem. *135*, 343–360. https://doi.org/10.1016/j.soilbio.2019.05.011.
5. Ren, L., Jensen, K., Porada, P., and Mueller, P. (2022). Biota-mediated carbon cycling—A synthesis of biotic-interaction controls on blue carbon. Ecol. Lett. *25*, 521–540. https://doi.org/10.1111/ele.13940.
6. Neumann, G., and Römheld, V. (2012). Rhizosphere chemistry in relation to plant nutrition. In Marschner's mineral nutrition of higher plants (Elsevier), pp. 347–368.
7. Kuzyakov, Y., and Blagodatskaya, E. (2015). Microbial hotspots and hot moments in soil: concept & review. Soil Biol. Biochem. *83*, 184–199. https://doi.org/10.1016/j.soilbio.2015.01.025.
8. Dijkstra, F.A., Zhu, B., and Cheng, W. (2021). Root effects on soil organic carbon: a double-edged sword. New Phytol. *230*, 60–65. https://doi.org/10.1111/nph.17082.
9. Oburger, E., and Jones, D.L. (2018). Sampling root exudates–mission impossible? Rhizosphere *6*, 116–133.
10. Neumann, G. (2007). Root exudates and nutrient cycling. In Nutrient cycling in terrestrial ecosystems (Springer), pp. 123–157.
11. Nguyen, C. (2009). Rhizodeposition of Organic C by Plant: Mechanisms and Controls (Springer). https://doi.org/10.1007/978-90-481-2666-8_9.
12. Eisenhauer, N., Lanoue, A., Strecker, T., Scheu, S., Steinauer, K., Thakur, M.P., and Mommer, L. (2017). Root biomass and exudates link plant diversity with soil bacterial and fungal biomass. Sci. Rep. *7*, 44641. https://doi.org/10.1038/srep44641.
13. Haichar, F.e.Z., Santaella, C., Heulin, T., and Achouak, W. (2014). Root exudates mediated interactions belowground. Soil Biol. Biochem. *77*, 69–80. https://doi.org/10.1016/j.soilbio.2014.06.017.
14. Canarini, A., Kaiser, C., Merchant, A., Richter, A., and Wanek, W. (2019). Root Exudation of Primary Metabolites: Mechanisms and Their Roles in Plant Responses to Environmental Stimuli. Front. Plant Sci. *10*, 157. https://doi.org/10.3389/fpls.2019.00157.
15. Gargallo-Garriga, A., Preece, C., Sardans, J., Oravec, M., Urban, O., and Peñuelas, J. (2018). Root exudate metabolomes change under drought and show limited capacity for recovery. Sci. Rep. *8*, 12696. https://doi.org/10.1038/s41598-018-30150-0.
16. Kuzyakov, Y., and Domanski, G. (2000). Carbon input by plants into the soil. Review. J. Plant Nutr. Soil Sci. *163*, 421–431. https://doi.org/10.1002/1522-2624(200008)163:4<421::AID-JPLN421>3.0.CO;2-R.
17. Jones, D.L., Hodge, A., and Kuzyakov, Y. (2004). Plant and mycorrhizal regulation of rhizodeposition. New Phytol. *163*, 459–480. https://doi.org/10.1111/j.1469-8137.2004.01130.x.
18. Pausch, J., and Kuzyakov, Y. (2018). Carbon input by roots into the soil: quantification of rhizodeposition from root to ecosystem scale. Global Change Biol. *24*, 1–12. https://doi.org/10.1111/gcb.13850.
19. Studer, M.S., Siegwolf, R.T.W., and Abiven, S. (2014). Carbon transfer, partitioning and residence time in the plant-soil system: a comparison of two 13 CO 2 labelling techniques. Biogeosciences *11*, 1637–1648. https://doi.org/10.5194/bg-11-1637-2014.
20. Meharg, A.A. (1994). A critical review of labelling techniques used to quantify

rhizosphere carbon-flow. Plant Soil *166*, 55–62. https://doi.org/10.1007/BF02185481.
21. Stevenel, P., Frossard, E., Abiven, S., Rao, I.M., Tamburini, F., and Oberson, A. (2019). Using a tri-isotope (^{13}C, ^{15}N, ^{33}P) labelling method to quantify rhizodeposition. Methods Rhizosphere Biol. Res. 169–195. https://doi.org/10.1007/978-981-13-5767-1_10.
22. Bais, H.P., Weir, T.L., Perry, L.G., Gilroy, S., and Vivanco, J.M. (2006). The role of root exudates in rhizosphere interactions with plants and other organisms. Annu. Rev. Plant Biol. *57*, 233–266. https://doi.org/10.1146/annurev.arplant.57.032905.105159.
23. Hirsch, A.M., Bauer, W.D., Bird, D.M., Cullimore, J., Tyler, B., and Yoder, J.I. (2003). Molecular signals and receptors: Controlling rhizosphere interactions between plants and other organisms. Ecology *84*, 858–868.
24. Wang, N.-Q., Kong, C.-H., Wang, P., and Meiners, S.J. (2021). Root exudate signals in plant-plant interactions. Plant Cell Environ. *44*, 1044–1058. https://doi.org/10.1111/pce.13892.
25. Rasmann, S., and Turlings, T.C. (2016). Root signals that mediate mutualistic interactions in the rhizosphere. Curr. Opin. Plant Biol. *32*, 62–68. https://doi.org/10.1016/j.pbi.2016.06.017.
26. Sun, Y., Wang, C., Yang, J., Liao, J., Chen, H.Y., and Ruan, H. (2021). Elevated CO_2 shifts soil microbial communities from K-to r-strategists. Global Ecol. Biogeogr. *30*, 961–972. https://doi.org/10.1111/geb.13281.
27. Samaras, A., Kamou, N., Tzelepis, G., Karamanoli, K., Menkissoglu-Spiroudi, U., and Karaoglanidis, G.S. (2022). Root transcriptional and metabolic dynamics induced by the plant growth promoting rhizobacterium (PGPR) Bacillus subtilis Mbi600 on cucumber plants. Plants *11*, 1218.
28. Herz, K., Dietz, S., Gorzolka, K., Haider, S., Jandt, U., Scheel, D., and Bruelheide, H. (2018). Linking root exudates to functional plant traits. PLoS One *13*, e0204128.
29. Schmid, M.W., Hahl, T., van Moorsel, S.J., Wagg, C., De Deyn, G.B., and Schmid, B. (2019). Feedbacks of plant identity and diversity on the diversity and community composition of rhizosphere microbiomes from a long-term biodiversity experiment. Mol. Ecol. *28*, 863–878. https://doi.org/10.1111/mec.14987.
30. Bais, H.P., Park, S.-W., Weir, T.L., Callaway, R.M., and Vivanco, J.M. (2004). How plants communicate using the underground information superhighway. Trends Plant Sci. *9*, 26–32. https://doi.org/10.1016/j.tplants.2003.11.008.
31. Bezerra, R.H.S., Sousa-Souto, L., Santana, A.E.G., and Ambrogi, B.G. (2021). Indirect plant defenses: volatile organic compounds and extrafloral nectar. Arthropod. Plant. Interact. *15*, 467–489. https://doi.org/10.1007/s11829-021-09837-1.
32. Rovira, A.D., and Harris, J.R. (1961). Plant root excretions in relation to the rhizosphere effect: v. The exudation of b-group vitamins. Plant Soil *14*, 199–214. https://doi.org/10.1007/BF01343852.
33. Streit, W.R., Joseph, C.M., and Phillips, D.A. (1996). Biotin and other water-soluble vitamins are key growth factors for alfalfa root colonization by Rhizobium meliloti 1021. Mol. Plant Microbe Interact. *9*, 330–338. https://doi.org/10.1094/mpmi-9-0330.
34. Phillips, D.A., and Streit, W. (1996). Legume signals to rhizobial symbionts: a new approach for defining rhizosphere colonization. In Plant-Microbe Interactions (Springer), pp. 236–271.
35. Hartmann, A., Rothballer, M., and Schmid, M. (2008). Lorenz Hiltner, a pioneer in rhizosphere microbial ecology and soil bacteriology research. Plant Soil *312*, 7–14. https://doi.org/10.1007/s11104-007-9514-z.
36. Ji, C., Liang, Z., Cao, H., Chen, Z., Kong, X., Xin, Z., He, M., Wang, J., Wei, Z., Xing, J., et al. (2023). Transcriptome-based analysis of the effects of compound microbial agents on gene expression in wheat roots and leaves under salt stress. Front. Plant Sci. *14*, 1109077. https://doi.org/10.3389/fpls.2023.1109077.
37. Timmusk, S., Paalme, V., Pavlicek, T., Bergquist, J., Vangala, A., Danilas, T., and Nevo, E. (2011). Bacterial distribution in the rhizosphere of wild barley under contrasting microclimates. PLoS One *6*, e17968.
38. Rudolph-Mohr, N., Tötzke, C., Kardjilov, N., and Oswald, S.E. (2017). Mapping water, oxygen, and pH dynamics in the rhizosphere of young maize roots. J. Plant Nutr. Soil Sci. *180*, 336–346. https://doi.org/10.1002/jpln.201600120.
39. Rüger, L., Feng, K., Dumack, K., Freudenthal, J., Chen, Y., Sun, R., Wilson, M., Yu, P., Sun, B., Deng, Y., et al. (2021). Assembly patterns of the rhizosphere microbiome along the longitudinal root axis of maize (Zea mays L.). Front. Microbiol. *12*, 614501. https://doi.org/10.3389/fmicb.2021.614501.
40. Kuzyakov, Y., and Schneckenberger, K. (2004). Review of estimation of plant rhizodeposition and their contribution to soil organic matter formation. Arch. Agron Soil Sci. *50*, 115–132. https://doi.org/10.1126/sciadv.abd3176.
41. Qiao, Y., Miao, S., Han, X., Yue, S., and Tang, C. (2017). Improving soil nutrient availability increases carbon rhizodeposition under maize and soybean in Mollisols. Sci. Total Environ. *603–604*, 416–424. https://doi.org/10.1016/j.scitotenv.2017.06.090.
42. Oburger, E., and Jones, D. (2009). Substrate mineralization studies in the laboratory show different microbial C partitioning dynamics than in the field. Soil Biol. Biochem. *41*, 1951–1956. https://doi.org/10.1016/j.soilbio.2009.06.020.
43. Dijkstra, F.A., Carrillo, Y., Pendall, E., and Morgan, J.A. (2013). Rhizosphere priming: a nutrient perspective. Front. Microbiol. *4*, 216. https://doi.org/10.3389/fmicb.2013.00216.
44. Zhang, X., Kuzyakov, Y., Zang, H., Dippold, M.A., Shi, L., Spielvogel, S., and Razavi, B.S. (2020). Rhizosphere hotspots: root hairs and warming control microbial efficiency, carbon utilization and energy production. Soil Biol. Biochem. *148*, 107872. https://doi.org/10.1016/j.soilbio.2020.107872.
45. Rolando, J.L., Kolton, M., Song, T., and Kostka, J.E. (2022). The core root microbiome of Spartina alterniflora is predominated by sulfur-oxidizing and sulfate-reducing bacteria in Georgia salt marshes, USA. Microbiome *10*, 37.
46. Cai, M., Yin, X., Tang, X., Zhang, C., Zheng, Q., and Li, M. (2022). Metatranscriptomics reveals different features of methanogenic archaea among global vegetated coastal ecosystems. Sci. Total Environ. *802*, 149848. https://doi.org/10.1016/j.scitotenv.2021.149848.
47. Su, W., Ye, C., Zhang, Y., Hao, S., and Li, Q.Q. (2019). Identification of putative key genes for coastal environments and cold adaptation in mangrove Kandelia obovata through transcriptome analysis. Sci. Total Environ. *681*, 191–201. https://doi.org/10.1016/j.scitotenv.2019.05.127.
48. Rolando, J.L., Kolton, M., Song, T., Liu, Y., Pinamang, P., Conrad, R., Morris, J.T., Konstantinidis, K.T., and Kostka, J.E. (2024). Sulfur oxidation and reduction are coupled to nitrogen fixation in the roots of the salt marsh foundation plant Spartina alterniflora. Nat. Commun. *15*, 3607. https://doi.org/10.1038/s41467-024-47646-1.
49. Carvalhais, L.C., Dennis, P.G., Tyson, G.W., and Schenk, P.M. (2013). Rhizosphere metatranscriptomics: challenges and opportunities. Mol Microbiol Ecol Rhizosphere *1*, 1137–1144. https://doi.org/10.1002/9781118297674.ch109.
50. Lu, Y., and Conrad, R. (2005). In situ stable isotope probing of methanogenic archaea in the rice rhizosphere. Science *309*, 1088–1090.
51. Megonigal, J.P., Hines, M., and Visscher, P. (2003). Anaerobic metabolism: linkages to trace gases and aerobic processes. Treatise Geochem *8*, 317–424. https://doi.org/10.1016/B0-08-043751-6/08132-9.
52. Keiluweit, M., Wanzek, T., Kleber, M., Nico, P., and Fendorf, S. (2017). Anaerobic microsites have an unaccounted role in soil carbon stabilization. Nat. Commun. *8*, 1771. https://doi.org/10.1038/s41467-017-01406-6.
53. Sutton-Grier, A.E., Keller, J.K., Koch, R., Gilmour, C., and Megonigal, J.P. (2011). Electron donors and acceptors influence anaerobic soil organic matter mineralization in tidal marshes. Soil Biol. Biochem. *43*, 1576–1583. https://doi.org/10.1016/j.soilbio.2011.04.008.
54. Yamauchi, T., Shimamura, S., Nakazono, M., and Mochizuki, T. (2013). Aerenchyma formation in crop species: a review. Field Crops Res. *152*, 8–16. https://doi.org/10.1016/j.fcr.2012.12.008.
55. Yang, S., Liebner, S., Walz, J., Knoblauch, C., Bornemann, T.L.V., Probst, A.J., Wagner, D., Jetten, M.S.M., and in 't Zandt, M.H. (2021). Effects of a long-term anoxic warming scenario on microbial community structure and functional potential of permafrost-affected soil. Permafr. Periglac. Process. *32*, 641–656. https://doi.org/10.1002/ppp.2131.
56. Akinyede, R., Taubert, M., Schrumpf, M., Trumbore, S., and Küsel, K. (2022). Dark CO_2 fixation in temperate beech and pine forest soils. Soil Biol. Biochem. *165*, 108526. https://doi.org/10.1016/j.soilbio.2021.108526.
57. Yang, Y., Yang, X., Gong, L., Ding, Z., Zhu, H., Tang, J., and Li, X. (2024). Changes in soil microbial carbon fixation pathways along the oasification process in arid desert region: A confirmation based on metagenome analysis. Catena *239*, 107955. https://doi.org/10.1016/j.catena.2024.107955.
58. Geng, H., Wang, F., Yan, C., Ma, S., Zhang, Y., Qin, Q., Tian, Z., Liu, R., Chen, H., Zhou, B., and Yuan, R. (2022). Rhizosphere microbial community composition and survival strategies in oligotrophic and metal (loid) contaminated iron tailings areas. J. Hazard Mater. *436*, 129045. https://doi.org/10.1016/j.jhazmat.2022.129045.
59. Momper, L., Jungbluth, S.P., Lee, M.D., and Amend, J.P. (2017). Energy and carbon metabolisms in a deep terrestrial subsurface fluid microbial community. ISME J. *11*, 2319–2333. https://doi.org/10.1038/ismej.2017.94.
60. Capone, D.G., and Kiene, R.P. (1988). Comparison of microbial dynamics in marine and freshwater sediments: Contrasts in anaerobic carbon catabolism. Limnol.

Oceanogr. *33*, 725–749. https://doi.org/10.4319/lo.1988.33.4part2.0725.

61. Jørgensen, B.B., Findlay, A.J., and Pellerin, A. (2019). The biogeochemical sulfur cycle of marine sediments. Front. Microbiol. *10*, 849. https://doi.org/10.3389/fmicb.2019.00849.
62. Lin, C.Y., Turchyn, A.V., Steiner, Z., Bots, P., Lampronti, G.I., and Tosca, N.J. (2018). The role of microbial sulfate reduction in calcium carbonate polymorph selection. Geochem. Cosmochim. Acta *237*, 184–204. https://doi.org/10.1016/j.gca.2018.06.019.
63. Grüterich, L., Woodhouse, J.N., Mueller, P., Tiemann, A., Ruscheweyh, H.-J., Sunagawa, S., Grossart, H.-P., and Streit, W.R. (2024). Environmental controls of dark CO_2 fixation in wetland microbiomes. Preprint at bioRxiv. https://doi.org/10.1101/2024.01.18.576062.
64. Dörries, M., Wöhlbrand, L., and Rabus, R. (2016). Differential proteomic analysis of the metabolic network of the marine sulfate-reducer Desulfobacterium autotrophicum HRM2. Proteomics *16*, 2878–2893. https://doi.org/10.1002/pmic.201600041.
65. Ragsdale, S.W., and Pierce, E. (2008). Acetogenesis and the Wood–Ljungdahl pathway of CO2 fixation. Biochim. Biophys. Acta *1784*, 1873–1898. https://doi.org/10.1016/j.bbapap.2008.08.012.
66. Bährle, R., Böhnke, S., Englhard, J., Bachmann, J., and Perner, M. (2023). Current status of carbon monoxide dehydrogenases (CODH) and their potential for electrochemical applications. Bioresour. Bioprocess. *10*, 84.
67. Li, Y., Jing, H., Xia, X., Cheung, S., Suzuki, K., and Liu, H. (2018). Metagenomic insights into the microbial community and nutrient cycling in the western subarctic Pacific Ocean. Front. Microbiol. *9*, 623. https://doi.org/10.3389/fmicb.2018.00623.
68. Crump, B.C., Peranteau, C., Beckingham, B., and Cornwell, J.C. (2007). Respiratory succession and community succession of bacterioplankton in seasonally anoxic estuarine waters. Appl. Environ. Microbiol. *73*, 6802–6810. https://doi.org/10.1128/AEM.00648-07.
69. Tebbe, D.A., Geihser, S., Wemheuer, B., Daniel, R., Schäfer, H., and Engelen, B. (2022). Seasonal and Zonal Succession of Bacterial Communities in North Sea Salt Marsh Sediments. Microorganisms *10*, 859. https://doi.org/10.3390/microorganisms10050859.
70. Lovley, D.R., Dwyer, D.F., and Klug, M.J. (1982). Kinetic analysis of competition between sulfate reducers and methanogens for hydrogen in sediments. Appl. Environ. Microbiol. *43*, 1373–1379. https://doi.org/10.1128/aem.43.6.1373-1379.1982.
71. Oremland, R.S., and Polcin, S. (1982). Methanogenesis and sulfate reduction: competitive and noncompetitive substrates in estuarine sediments. Appl. Environ. Microbiol. *44*, 1270–1276. https://doi.org/10.1128/aem.44.6.1270-1276.1982.
72. Poffenbarger, H. (2010). Ruminant grazing of cover crops: Effects on soil properties and agricultural production. J. Nat. Resour. Life Sci. Educ. *39*, 49-39. https://doi.org/10.4195/jnrlse.2010.0003se.
73. Büttner, D. (2016). Behind the lines–actions of bacterial type III effector proteins in plant cells. FEMS Microbiol. Rev. *40*, 894–937. https://doi.org/10.1093/femsre/fuw026.
74. Kloock, A., Bonsall, M.B., and King, K.C. (2020). Evolution and maintenance of microbe-mediated protection under occasional pathogen infection. Ecol. Evol. *10*, 8634–8642. https://doi.org/10.1002/ece3.6555.
75. Chiang, S.M., and Schellhorn, H.E. (2012). Regulators of oxidative stress response genes in Escherichia coli and their functional conservation in bacteria. Arch. Biochem. Biophys. *525*, 161–169. https://doi.org/10.1016/j.abb.2012.02.007.
76. Huang, H., Ullah, F., Zhou, D.-X., Yi, M., and Zhao, Y. (2019). Mechanisms of ROS regulation of plant development and stress responses. Front. Plant Sci. *10*, 800. https://doi.org/10.3389/fpls.2019.00800.
77. Tan, S., Yang, C., Mei, X., Shen, S., Raza, W., Shen, Q., and Xu, Y. (2013). The effect of organic acids from tomato root exudates on rhizosphere colonization of Bacillus amyloliquefaciens T-5. Appl. Soil Ecol. *64*, 15–22. https://doi.org/10.1016/j.apsoil.2012.10.011.
78. Wu, X., Bei, S., Zhou, X., Luo, Y., He, Z., Song, C., Yuan, H., Pivato, B., Liesack, W., and Peng, J. (2023). Metagenomic insights into genetic factors driving bacterial niche differentiation between bulk and rhizosphere soils. Sci. Total Environ. *891*, 164221. https://doi.org/10.1016/j.scitotenv.2023.164221.
79. Verhagen, F.J.M., Laanbroek, H.J., and Woldendrop, J.W. (1995). Competition for ammonium between plant roots and nitrifying and heterotrophic bacteria and the effects of protozoan grazing. Plant Soil *170*, 241–250. https://doi.org/10.1007/BF00010477.
80. Tollerson, R., and Ibba, M. (2020). Translational regulation of environmental adaptation in bacteria. J. Biol. Chem. *295*, 10434–10445. https://doi.org/10.1074/jbc.REV120.012742.
81. Yang, J., Tam, N.F.-Y., and Ye, Z. (2014). Root porosity, radial oxygen loss and iron plaque on roots of wetland plants in relation to zinc tolerance and accumulation. Plant Soil *374*, 815–828. https://doi.org/10.1007/s11104-013-1922-7.
82. Chen, Y.-T., Wang, Y., and Yeh, .K-C. (2017). Role of root exudates in metal acquisition and tolerance. Curr. Opin. Plant Biol. *39*, 66–72.
83. Nuccio, E.E., Starr, E., Karaoz, U., Brodie, E.L., Zhou, J., Tringe, S.G., Malmstrom, R.R., Woyke, T., Banfield, J.F., Firestone, M.K., and Pett-Ridge, J. (2020). Niche differentiation is spatially and temporally regulated in the rhizosphere. ISME J. *14*, 999–1014. https://doi.org/10.1038/s41396-019-0582-x.
84. Borges, F.O., Santos, C.P., Paula, J.R., Mateos-Naranjo, E., Redondo-Gomez, S., Adams, J.B., Caçador, I., Fonseca, V.F., Reis-Santos, P., Duarte, B., and Rosa, R. (2021). Invasion and extirpation potential of native and invasive Spartina species under climate change. Front. Mar. Sci. *8*, 696333. https://doi.org/10.3389/fmars.2021.696333.
85. Kieser, S., Brown, J., Zdobnov, E.M., Trajkovski, M., and McCue, L.A. (2020). ATLAS: a Snakemake workflow for assembly, annotation, and genomic binning of metagenome sequence data. BMC Bioinf. *21*, 1–8.
86. Nurk, S., Meleshko, D., Korobeynikov, A., and Pevzner, P.A. (2017). metaSPAdes: a new versatile metagenomic assembler. Genome Res. *27*, 824–834. https://doi.org/10.1101/gr.213959.116.
87. Cantalapiedra, C.P., Hernández-Plaza, A., Letunic, I., Bork, P., and Huerta-Cepas, J. (2021). eggNOG-mapper v2: functional annotation, orthology assignments, and domain prediction at the metagenomic scale. Mol. Biol. Evol. *38*, 5825–5829. https://doi.org/10.1093/molbev/msab293.
88. Wu, Y.-W., Simmons, B.A., and Singer, S.W. (2016). MaxBin 2.0: an automated binning algorithm to recover genomes from multiple metagenomic datasets. Bioinformatics *32*, 605–607. https://doi.org/10.1093/bioinformatics/btv638.
89. Kang, D.D., Li, F., Kirton, E., Thomas, A., Egan, R., An, H., and Wang, Z. (2019). MetaBAT 2: an adaptive binning algorithm for robust and efficient genome reconstruction from metagenome assemblies. PeerJ *7*, e7359. https://doi.org/10.7717/peerj.7359.
90. Sieber, C.M.K., Probst, A.J., Sharrar, A., Thomas, B.C., Hess, M., Tringe, S.G., and Banfield, J.F. (2018). Recovery of genomes from metagenomes via a dereplication, aggregation and scoring strategy. Nat. Microbiol. *3*, 836–843. https://doi.org/10.1038/s41564-018-0171-1.
91. Parks, D.H., Imelfort, M., Skennerton, C.T., Hugenholtz, P., and Tyson, G.W. (2015). CheckM: assessing the quality of microbial genomes recovered from isolates, single cells, and metagenomes. Genome Res. *25*, 1043–1055. https://doi.org/10.1101/gr.186072.114.
92. Chaumeil, P.-A., Mussig, A.J., Hugenholtz, P., and Parks, D.H. (2019). GTDB-Tk: a toolkit to classify genomes with the Genome Taxonomy Database. Bioinformatics *36*, 1925–1927. https://doi.org/10.1093/bioinformatics/btz848.
93. Li, H. (2021). New strategies to improve minimap2 alignment accuracy. Bioinformatics *37*, 4572–4574.
94. Love, M.I., Huber, W., and Anders, S. (2014). Moderated estimation of fold change and dispersion for RNA-seq data with DESeq2. Genome Biol. *15*, 1–21. https://doi.org/10.1186/s13059-014-0550-8.
95. Granse, D., Titschack, J., Ainouche, M., Jensen, K., and Koop-Jakobsen, K. (2022). Subsurface aeration of tidal wetland soils: Root-system structure and aerenchyma connectivity in Spartina (Poaceae). Sci. Total Environ. *802*, 149771. https://doi.org/10.1016/j.scitotenv.2021.149771.

STAR★METHODS

KEY RESOURCES TABLE

REAGENT or RESOURCE	SOURCE	IDENTIFIER
Biological samples		
Soil used for plant cultivation	Hamburger Hallig, Germany (54°36′06.2″N, 103 8°49′00.1″E)	N/A
Deposited data		
Raw sequence data	This Paper	ENA: PRJEB73855
Experimental models: Organisms/strains		
Spartina anglica	Hamburger Hallig, Germany (54°36′06.2″N, 103 8°49′00.1″E)	N/A
Software and algorithms		
ATLAS pipeline v2.12.0	Kieser et al., 2020[85]	https://github.com/metagenome-atlas/atlas
metaSPAdes v3.15.3	Nurk et al., 2017[86]	https://kbase.us/applist/apps/kb_SPAdes/run_metaSPAdes/release
eggNOG mapper v2.1	Cantalapiedra et al., 2021[87]	http://eggnog-mapper.embl.de/
eggNOG database v5.0	Cantalapiedra et al., 2021[87]	http://eggnog5.embl.de/#/app/home
maxBin2 v2.2	Wu et al., 2016[88]	https://github.com/upendrak/MaxBin-2.2/blob/master/Dockerfile
metabat2 v2.15	Kang et al., 2019[89]	https://bioweb.pasteur.fr/packages/pack@MetaBAT@2.15
DAS_Tool v1.1.4	Sieber et al., 2018[90]	https://github.com/cmks/DAS_Tool/releases
checkM v1.1.10	Parks et al., 2015[91]	https://github.com/Ecogenomics/CheckM/releases
GTDBtk tool v2.1.1	Chaumeil et al., 2020[92]	https://software.cqls.oregonstate.edu/updates/gtdbtk-2.1.1/
minimap2 v2.14	Li, 2021[93]	https://github.com/lh3/minimap2
DESeq2 package v1.34	Love et al., 2014[94]	https://bioconductor.org/packages/release/bioc/html/DESeq2.html

EXPERIMENTAL MODEL AND STUDY PARTICIPANT DETAILS

Spartina anglica plant cultivation

Spartina anglica (also known as *Sporobolus anglicus*) is a common salt marsh plant along the European Atlantic coast.[95] It is the direct allopolyploid descendant of the hybrid *Spartina x townsendii*, which formed in Southern England by hybridization between native *S. maritima* and the introduced *S. alterniflora* (originating from North America) at the end of the 19th century. All individuals of *Spartina anglica* and soil were sampled in June of 2021 from the pioneer zone of a Wadden Sea salt marsh situated at the Hamburger Hallig (54°36′06.2″N, 103 8°49′00.1″E) and cultivated thereafter in a greenhouse on a mixture of native pioneer zone soil, sand and fertilizer until the start of experimentation at the Institute of Plant Science and Microbiology (University of Hamburg, Hamburg, Germany). Plants were given several weeks to adapt to greenhouse conditions upon sampling from the field. Two weeks prior to pulse labeling, three individuals of similar size and vitality (new shoot growth was observed) were rinsed and transferred into non-transparent plant pots without fertilizer and filled only with freshly homogenized and sieved native soil (pioneer zone; Hamburger Hallig). All pots, including unplanted control pots, were kept under waterlogged conditions prior to and during pulse labeling.

METHOD DETAILS

To evaluate the influence of root activity and, particularly, exudate input on soil microbial gene expression, we conducted a $^{13}CO_2$ pulse labeling experiment and traced the flux of recently formed photo-assimilates into the rhizosphere. We used the ^{13}C signal of soil samples as a proxy for the presence of root exudates (Figure S2) and distinguished soil and rhizosphere micro-environments that received root exudates (n = 3) from those that did not (n = 3) using isotope-ratio mass spectrometry. We conducted metatranscriptome sequencing of the soil microbial RNA (of bacteria and archaea) and employed both functional annotation and a differential expression analysis for N = 6 metatranscriptomes.

$^{13}CO_2$ pulse labeling

We used a plexiglass cylinder (thickness: 3 mm, diameter: 200/194 mm, height: 45 cm) with a removable lid to construct a labeling chamber. The chamber was equipped with a fan for air mixing and a sensor measuring atmospheric CO_2, temperature, and humidity (K33 LP T/RH Sensor; Senseair). The sensor was connected to an Arduino computer outside the chamber, which recorded the data on an SD card. Only the aboveground plant biomass was placed inside the chamber for $^{13}CO_2$ labeling and was sealed around the shoot base using clamps and plastic film (Figure S1). $^{13}CO_2$ was produced inside the chamber by adding 8 mL of 10% HCl to 0.1 g $NaH^{13}CO_3$ (Sigma-Aldrich, St. Louis, USA). We used a 300-W LED light (Roleadro) as a light source for plant photosynthesis (Figure S1). Plants were labeled daily over eight consecutive days. Label duration was 2–3 h and dependent on the time it took for the plants to draw chamber CO_2 concentrations (>1500 ppm) well below atmospheric concentrations (250–350 ppm).

Soil sample collection and ^{13}C enrichment analysis

After eight days of daily pulse-labeling, intact soil sods (2 L) extracted from three planted pots and one unplanted control pot were vertically separated into two-halves exposing the soils and rhizospheres for sampling. 10 soil subsamples (approximately 1.5 cm^3) were collected from each soil sod at random positions along a transect from the bulk soil toward the root mass using a spatula (N = 40). Subsequently, all 40 soil samples were frozen in 2-mL cryotubes using liquid nitrogen and stored at −80°C until further processing.

Soil samples were dried at 60°C to constant weight and ground using a ball mill (Retsch, Haan, Germany). Carbonates were removed through direct acidification of the soil samples using 10% HCl. Samples were weighed into tin capsules and analyzed for their isotopic ^{13}C signatures using an element analyzer (EURO-EA 3000, Euro Vector, Pavia, Italy) coupled to an isotope-ratio mass spectrometer (Nu Horizon, Nu Instruments, Wrexham, United Kingdom). Among these 40 samples, bulk and rhizosphere soil samples were not pre-determined by their proximity to the root but were operationally defined by their ^{13}C signature. Soil samples with isotopically enriched ^{13}C signatures were defined as impacted by root exudates, i.e., rhizosphere soil, whereas soil samples that showed no indication of ^{13}C enrichment in relation to control soils were defined as not affected by exudates, i.e., bulk soil. All soil samples were ranked by their ^{13}C enrichment in relation to control soils, and samples with the greatest ^{13}C enrichment (n = 3) were compared to samples that showed no ^{13}C divergence from the control (n = 3).

RNA and DNA extraction from soil

2 g of soil were used for RNA extraction using the RNeasy PowerSoil Kit (Qiagen, Venlo, Netherlands) following the manufacturer's protocol. RNA concentrations were quantified using the Qubit 2.0 Fluorometer and the RNA High Sensitivity Assay Kit (RNA HS, Thermo Fisher, Berlin, Germany). To efficiently assign the RNA sequences to the respective genes, we also sequenced the DNA of two soil samples (one from the rhizosphere and one from the unplanted soil). DNA was extracted from soil samples, and frozen at −80°C until analysis. 0.5 g of soil were used for DNA extraction using the NucleoSpin Soil Kit (Macherey-Nagel, Düren, Germany) following the manufacturer's protocol. Subsequently, the isolated DNA was analyzed at a wavelength of 280 nm using a Nanodrop spectrophotometer (NanoDrop 2000, Thermo Scientific, Waltham, USA).

Metatranscriptome and metagenome analysis

First, the two metagenomes were combined and co-assembled. We used the ATLAS pipeline v2.12.0[85] that includes an extended workflow for quality control, contig assembly, gene prediction and functional annotation, binning of contigs into MAGs and taxonomic annotation of the MAGs. Among the included tools are several gold-standard tools, e.g., metaSPAdes v3.15.3 for read assembly[86], eggNOG mapper v2.1 and eggNOG database v5.0 for functional gene annotation,[87] maxBin2 v2.2, metabat2 v2.15 and DAS_Tool v1.1.4 for binning and refinement of MAGs,[88–90] checkM v1.1.10 for MAG quality assesment[91] and GTDBtk tool v2.1.1 with GTDB database release207 for taxonomic annotation of the MAGs.[92] Default parameters were used, except for RAM (up to 1.5 TB) and CPU/threads (up to 80 threads). The co-assembled metagenome had a total of 38 million reads assembled into 87362 contigs with an N50 value of 14,475 (Figure S1). 13 MAGs with contamination <10% and with completeness between 70 and 99.8% were extracted. Second, the metagenome data for individual samples were quality controlled using the ATLAS pipeline and the high-quality reads were mapped to the MAGs from the co-assembly using minimap2 v2.14[93] to assess the abundance of the MAGs within the single samples (Table S2). Third, metatranscriptomes were quality controlled using the ATLAS pipeline and high-quality reads were mapped to the genes detected on the assembled contigs from the metagenome co-assembly using minimap2 v2.14.[93] Differential genes expression analysis was performed using R 4.0 and DESeq2 package v1.34.[94] Transcript counts were normalized using the RPM (read per million mapped reads) normalization method to correct for different sequencing depth between the sample. One sample (S3_10_low) has low total reads (Table S2), but this should be accounted for by DESeq normalization and reflected by a poorer p-value.

Future studies could increase sequencing depth to 40 million reads for better data accuracy. To reduce the large proportion of eukaryotic reads, removing polyA-tailed RNA during library preparation may enrich prokaryotic RNA.

QUANTIFICATION AND STATISTICAL ANALYSIS

All transcriptomes were filtered for only prokaryotic reads, to exclude reads that were assigned to the plant. We did this by employing the ATLAS pipeline, which includes the metaSPAdes tool optimized specifically for prokaryotic reads filtering. Despite the more complex

gene structures of eukaryotes, such as exons and introns, making gene prediction more challenging, parts of eukaryotic genes could still be predicted and annotated by eggNOG. Subsequently, in the second step, we removed all gene queries annotated to eukaryota. This constituted 0.38% of all gene queries with at least one transcript assigned. Further, 3.77% of all gene queries could not be taxonomically assigned (Figure S3). Since these genes also could not be functionally assigned, they were excluded from the key gene analysis (Figure 3) and the differential expression analyses where we investigated the impact of root exudates on soil microbes (Figure 5). With this we ensured to only analyze the response of bacteria and archaea to root influence. The selection of genes for the key gene analysis (Figure 3) was modified after Yang et al.,[55] to cover the carbon, nitrogen and sulfur cycling of anoxic ecosystems. We additionally added key genes of dark CO_2 fixation. The key gene analysis is based on all transcripts independent of differential expression. The given transcript abundances depict the average of six metatranscriptomes.

For identification of differentially expressed genes, we applied an adjusted *p*-value <0.05 and a $\log_2$ fold change >2, < −2. To investigate which metabolic pathways are upregulated and which are downregulated in response to plant exudate influence, pathway annotation was performed on genes with a significant change in gene expression ($p < 0.05$) based on the "Kyoto Encyclopedia of Genes and Genomes" (KEGG) database and complemented by in depth literature search in order to cover most of the genes, that could not be assigned through the KEGG database. The distribution of all differentially expressed genes assigned to a given pathway subcategory was visualized in a box and whisker plot in the style of Tukey. All data points that extend beyond 1.5 * IQR of the upper hinge (upper whisker) or below 1.5 * IQR of the lower hinge (lower whisker) are defined as outliers.